THE FASEB JOURNAL • RESEARCH • www.fasebj.org

ZBED6 negatively regulates insulin production, neuronal differentiation, and cell aggregation in MIN6 cells

Xuan Wang,[*,1] Lin Jiang,[†,‡,1] Ola Wallerman,[§] Shady Younis,[†,¶] Qian Yu,[*] Axel Klaesson,[†] Anders Tengholm,[*] Nils Welsh,[*,2] and Leif Andersson[†,§,3]

[*]Department of Medical Cell Biology and [†]Department of Medical Biochemistry and Microbiology, Science for Life Laboratory, Uppsala University, Uppsala, Sweden; [‡]The Key Laboratory for Farm Animal Genetic Resources and Utilization of Ministry of Agriculture of China, Institute of Animal Science, Chinese Academy of Agricultural Sciences, Beijing, China; [§]Department of Animal Breeding and Genetics, Swedish University of Agricultural Sciences, Uppsala, Sweden; and [¶]Department of Animal Production, Ain Shams University, Shoubra El-Kheima, Cairo, Egypt

ABSTRACT: Zinc finger BED domain containing protein 6 (*Zbed6*) has evolved from a domesticated DNA transposon and encodes a transcription factor unique to placental mammals. The aim of the present study was to investigate further the role of ZBED6 in insulin-producing cells, using mouse MIN6 cells, and to evaluate the effects of Zbed6 knockdown on basal β-cell functions, such as morphology, transcriptional regulation, insulin content, and release. *Zbed6*-silenced cells and controls were characterized with a range of methods, including RNA sequencing, chromatin immunoprecipitation sequencing, insulin content and release, subplasma membrane Ca^{2+} measurements, cAMP determination, and morphologic studies. More than 700 genes showed differential expression in response to *Zbed6* knockdown, which was paralleled by increased capacity to generate cAMP, as well as by augmented sub-plasmalemmal calcium concentration and insulin secretion in response to glucose stimulation. We identified >4000 putative ZBED6-binding sites in the MIN6 genome, with an enrichment of ZBED6 sites at upregulated genes, such as the β-cell transcription factors v-maf musculoaponeurotic fibrosarcoma oncogene homolog A and Nk6 homeobox 1. We also observed altered morphology/growth patterns, as indicated by increased cell clustering, and in the appearance of axon-like Neurofilament, medium polypeptide and tubulin β 3, class III-positive protrusions. We conclude that ZBED6 acts as a transcriptional regulator in MIN6 cells and that its activity suppresses insulin production, cell aggregation, and neuronal-like differentiation.—Wang, X., Jiang, L., Wallerman, O., Younis, S., Yu, Q., Klaesson, A., Tengholm, A., Welsh, N., Andersson, L. ZBED6 negatively regulates insulin production, neuronal differentiation, and cell aggregation in MIN6 cells. FASEB J. 33, 000–000 (2019). www.fasebj.org

KEY WORDS: β-cells · cell adhesion · transcriptome analysis · ChIP-seq

ABBREVIATIONS: AC, adenylyl cyclase; Cdh, cadherins; ChIP-seq, chromatin immunoprecipitation sequencing; DAVID, Database for Annotation, Visualization and Integrated Discovery; DE, differentially expressed; FDR, false discovery rate; GO, gene ontology; IBMX, 3-isobutyl-1-methylxanthine; IGF2, Insulin like growth factor II; Isl1, ISL1 transcription factor, LIM/homeodomain; MafA, v-maf musculoaponeurotic fibrosarcoma oncogene homolog A; MEME, multiple EM for motif elicitation; Nefl, Neurofilament, light polypeptide; NEFM, Neurofilament, medium polypeptide; Nkx6-1, Nk6 homeobox 1; Pcdh, protocadherins; PDE, phosphodiesterase; Pdx1, pancreatic and duodenal homeobox 1; qPCR, quantitative PCR; RefSeq, Reference Sequence; RPKM, reads per kilobase per million mapped reads; sh, short hairpin; TSS, transcription start site; Tubb3, tubulin β 3, class III; WT, wild type; ZBED6, zinc finger BED domain-containing protein 6

[1] These authors contributed equally to this work.
[2] Correspondence: Department of Medical Cell Biology, Science for Life Laboratory, Uppsala University, Husargatan 3, Box 571, BMC, SE-751 23 Uppsala, Sweden. E-mail: nils.welsh@mcb.uu.se
[3] Correspondence: Department of Medical Biochemistry and Microbiology, Science for Life Laboratory, Uppsala University, Box 582, SE-751 23 Uppsala, Sweden. E-mail: leif.andersson@imbim.uu.se

doi: 10.1096/fj.201600835R
This article includes supplemental data. Please visit *http://www.fasebj.org* to obtain this information.

The zinc finger BED domain-containing protein 6 (ZBED6) is a recently discovered transcription factor, which is unique to and highly conserved among all placental mammals (1). The high sequence conservation of its dimerization and DNA-binding domains in placental mammals, but not in marsupials, suggests that *Zbed6* has evolved an essential function after the split between marsupials and Eutherian mammals (2). ZBED6 has a validated binding site in intron 3 of the Igf2 gene, and it acts as a repressor at this site in muscle cells (1, 3). A single nucleotide substitution at the ZBED6-binding site in intron 3 of *Igf2* in pigs abrogates the binding of ZBED6 and leads to increased *IGF2* expression, resulting in increased muscle growth and reduced subcutaneous fat depth. Also in mice, ZBED6 binding to its site in the *Igf2* gene reduces IGF2 levels in adult tissues and therefore, also the growth of muscle and internal organs (4).

It was previously reported that defective IGF2 production in the embryonic pancreas preceded the subsequent β-cell mass anomaly that develops in the diabetic rat (5),

w.fasebj.org by The University of British Columbia Library (142.103.160.110) on July 28, 2018. The FASEB Journal Vol. ${article.issue.getVolume()}, No. ${article.issue.getIssueNum

Furthermore, IGF2 overexpression in β-cells promotes cellular dysfunction *in vitro* (6) and diabetes in mice (7). Interestingly, it has recently been observed that a loss-of-function splice acceptor variant in the *Igf2* gene protects against type 2 diabetes (8). The splice acceptor variant reduced expression of IGF2 isoform 2, suggesting that IGF2 modulates the risk of type 2 diabetes in humans (8). Thus, ZBED6, *via* control of IGF2 expression, controls not only muscle growth but also may modulate events related to insulin production and sensitivity. In further support for a role of ZBED6 in β-cells, chromatin immunoprecipitation sequencing (ChIP-seq) identified >1200 genes with ZBED6-binding sites in C2C12 cells (1). Several genes encoding master transcription factors in β-cell maturation, such as v-maf musculoaponeurotic fibrosarcoma oncogene homolog A (*Mafa*), Neurogenin 3 (*Neurog3*), Neurogenic differentiation 2 (*Neurod2*), and Nk6 homeobox 1 (*Nkx6-1*), were among the genes bound by ZBED6 in C2C12 cells. Therefore, ZBED6 may play a significant role during β-cell development and as a consequence, might be pertinent to the pathogenesis of various types of diabetes mellitus.

We have recently observed that knockdown of *Zbed6* in mouse β-TC6 cells resulted in increased insulin production and decreased proliferation rates (9). Therefore, the aim of the present study was to investigate further the role of ZBED6 in insulin-producing cells, using mouse MIN6 cells, and to evaluate the effects on ZBED6 knockdown on basal β-cell functions, such as morphology, transcriptional regulation, insulin content, and release.

MATERIALS AND METHODS

Cell culture

MIN6 cells (passage 20–35) were maintained in DMEM with 15% fetal calf serum, 2 mM L-glutamine, 70 μM 2-ME, streptomycin (0.1 mg/ml), and benzylpenicillin (100 U/ml) at 37°C in a humidified atmosphere with 5% CO_2. In some experiments, MIN6 cells were cultured on culture plates coated with 10 μg/ml mouse laminin (Thermo Fisher Scientific, Waltham, MA, USA).

Generation of stable ZBED6-shRNA MIN6 cell lines

Short hairpin (sh) sequences against the *Zbed6* gene were cloned into lentiviral vectors and used for MIN6 cell transduction, as previously described (9). Two target sequences were used (ZBED6-sh1: 5′-CTTCAACACTTCAACGACA-3′ and ZBED6-sh2: 5′-TGTGGTACATGCAATCAAA-3′), and cells with stable shZBED6 expression were selected by puromycin (10 μg/ml) for at least 2 wk. Control cells (shMock) were transduced with virus carrying a scrambled shRNA sequence. Multiple cell clones from the shMock, sh1, and sh2 treatments were pooled to generate the 3 mixed cell populations, which minimizes the risk of random clonal selection.

ChIP-seq

Cells were crosslinked with 1% formaldehyde for 10 min, quenched with glycine, and stored at −80°C. After thawing and treatment with cell lysis buffer, chromatin was sonicated in RIPA buffer using a BioRuptor (40 min with 30 s on/off cycles in 2 × 750 μl buffer). Two separate ChIPs were prepared on chromatin from 66 and 10 million cells, respectively, using 20 μl Dynal Protein G Beads with 2 μg ZBED6 antibody. NEXTflex adaptors (Bioo Scientific, Austin, TX, USA) were used for library preparation with enzymes from Thermo Fisher Scientific (Fast End Repair, 25 μl for 15 min, 1 μl Klenow exo-minus DNA polymerase for 30 min at 37°C, 0.5 μl fast ligase for 15 min) before sequencing on an Illumina HiSeq2000. Reads were aligned to the mouse mm9 assembly using Burrows-Wheeler Aligner v.0.5.9, SAMtools (10) were used to remove alignments with low-alignment quality (<20), and a MIN6 input sample (E-MTAB-1143) was used as a control in peak calling using model-based analysis of ChIP-seq version 1.41 with merged reads from both replicates. All reads were used in peak calling to avoid saturated peaks. Motifs of 6–20 bp length were identified with multiple EM for motif elicitation (MEME)-ChIP (11) in 200 bp sequences centered on the summits of the 500 highest peaks.

RNA sequencing

RNA from shMock and sh1 MIN6 cells was isolated using the RNeasy mini kit (Qiagen, Germantown, MD, USA) and were further enriched for mRNA with MicroPoly (A) Purist (Ambion, Austin, TX, USA). The quality and quantity of the mRNA triplicates for each treatment were evaluated with a Bioanalyzer 2100 (Agilent Technologies, Santa Clara, CA, USA), and 0.5–1 μg mRNA for each sample was used for RNA sequencing (Illumina HiSeq 2000 platform) with the ScriptSeq protocol. Paired-end pooled sequencing of 6 barcoded samples (3 independent samples of each cell type) was done on 2 lanes, and reads were aligned to mm9 using TopHat 2.0.4 (12). The Cufflinks package v2.0.2 (13) with Reference Sequence (RefSeq) genes was used for differential expression analysis.

Gene ontology analysis

The official gene symbols of the differentially expressed (DE) genes were submitted to the Database for Annotation, Visualization and Integrated Discovery (DAVID) Bioinformatics Resources 6.7 (*http://david.abcc.ncifcrf.gov/*) for the functional annotation chart analysis with default settings for gene ontology (GO) analysis. A false-discovery rate (FDR)-corrected $P < 0.05$ and fold enrichment >2.5 were used to identify significantly enriched GO categories.

DNA constructs and reporter gene activity assays

The promoter sequences that showed high-transcription activities in pancreatic tissues of the 3 genes [pancreatic and duodenal homeobox 1 (*Pdx1*), *Nkx6-1*, and *Mafa*] were extracted from the FANTOM5 database (14). These promoter sequences that harbor the putative ZBED6-binding sites were cloned into the pGL4.15 [luc2P/Hygro] vector (Promega, Madison, WI, USA). The *Pdx1* construct contained a 680 bp insert [chr5:147,269,967–147,270,646, mouse Dec. 2011 (GRCm38/mm10) assembly] with 5 putative ZBED6-binding sites, the *Nkx6-1* construct contained a 700 bp insert [chr5:101,664,577–101,665,276, mouse Dec. 2011 (GRCm38/mm10) assembly] with 6 binding sites, and the *Mafa* construct contained a 600 bp insert [chr15:75,747,747–75,748,346, mouse Dec. 2011 (GRCm38/mm10) assembly] with 3 binding sites. The differences between the wild-type (WT) and mutant constructs are the substitution of an A for G at the ZBED6 consensus motif 5′-GCTCG-3′ in the cloned insert (15). MIN6 cells were cultured in a 24-well plate and then cotransfected with 750 ng DNA constructs and 50 ng *Renilla* vector, ph-RG-TK (Promega) using Opti-MEM I Reduced Serum Media, and Lipofectamine 3000 (Thermo Fisher Scientific). Cells were incubated for 36 h, and luciferase activity was measured using the Dual Luciferase Reporter Assay Kit (Promega) and an Infinite M200 Luminometer (Tecan, Männedorf, Switzerland).

w.fasebj.org by The University of British Columbia Library (142.103.160.110) on July 28, 2018. The FASEB Journal Vol. ${article.issue.getVolume()}, No. ${article.issue.getIssueNum

Luciferase activity was expressed as relative luciferase units (*Firefly*/*Renilla* luciferase activity). The differences between the WT and mutant sequences activities were considered significant at $P < 0.05$ of Student's t test with 2-tailed distribution, $n = 4$ experiments.

Insulin release and total insulin content measurement

Stable ZBED6-shRNA and shMock MIN6 cells (1×10^5 cells/well, 24-well plate) were seeded and precultured in DMEM for 2 d. Insulin contents were measured, as previously described (9). For insulin release determinations, the cells were preincubated for 30 min in 4-2-hydroxyethyl)-1-piperazineethanesulfonic acid-balanced Krebs-Ringer bicarbonate buffer (9) containing 0.2% bovine serum albumin and 1.67 mM D-glucose and then incubated for 1 h with 1.67 or 16.7 mM glucose or 30 mM KCl combined with 1.67 mM glucose. Insulin concentrations were measured by the Mercodia Insulin ELISA Kit (Mercodia AB, Uppsala, Sweden). The amount of insulin was normalized by cell number, as assessed by flow cytometry.

Measurements of the subplasma membrane Ca^{2+} concentration

Cells were seeded onto a 25 mm coverslip at a density of 2×10^5 cells per glass. After overnight culture, the cells were loaded with a Ca^{2+} indicator by 30 min incubation at 37°C in experimental buffer containing 125 mM NaCl, 4.8 mM KCl, 1.3 mM $CaCl_2$, 1.2 mM $MgCl_2$, 25 mM 4-(2-hydroxyethyl)-1-piperazineethanesulfonic acid (pH 7.40), and 1.67 mM glucose and supplemented with 1.5 μM Fluo-5F-acetoxymethyl ester (Thermo Fisher Scientific). After rinsing the cells in indicator-free buffer, the coverslip was mounted in a superfusion chamber on the stage of a custom-built total internal reflection fluorescence microscopy setup, previously described (16). The system was based on an E600FN (Nikon, Tokyo, Japan) upright microscope contained in an acrylic glass box thermostated at 37°C. Fluo-5F fluorescence was excited by a 491 nm diode-pumped, solid-state laser (Cobolt) and detected through a 16×, 0.8 numerical aperture water-immersion objective at 530 nm (50 nm half-bandwidth) with a digital camera (Orca-AG, Hamamatsu, Japan) under the control of MetaFluor software (Molecular Devices, Sunnyvale, CA, USA). Images were acquired every 3 s. Changes in fluorescence intensity over time were recorded from manually defined regions of interest corresponding to individual cells. The data were normalized by expressing the fluorescence relative to the prestimulatory intensity after background subtraction. Time-average Ca^{2+} levels were calculated by measuring the area under the curve, followed by normalization for the elapsed time.

Measurements of cAMP content in response to forskolin and IBMX

MIN6 cells in 6-well plates were incubated in DMEM culture medium with the addition of 10 μM forskolin and 100 μM 3-isobutyl-1-methylxanthine (IBMX) for 20 min. The cAMP levels were measured by the cAMP ELISA Kit (Cayman Chemical, Ann Arbor, MI, USA), according to the manufacturer's instructions.

Real-time semiquantitative RT-PCR

Isolation of RNA and cDNA synthesis was performed as previously described (9). The mRNA transcripts were measured by semi-quantitative PCR (qPCR) analysis using the SYBR Green Taq Readymix (MilliporeSigma, St. Louis, MO, USA) on a Light Cycler 2.0 instrument (Roche, Basel, Switzerland) (9). We used 18S and β-actin as housekeeping genes. Data were normalized by using the average C_t value of these 2 endogenous controls and further analyzed by the $2-\Delta\Delta C_t$ method. Sequences of the primers are given in Supplemental Table S1.

Immunoblot analysis

Immunoblot analysis was performed as previously described (9) using the following antibodies: ZBED6 (1:1000), PDX1 (1:1000; Cell Signaling Technology, Danvers, MA, USA), α-tubulin (1:1000; Santa Cruz Biotechnology, Dallas, TX, USA), and Neurofilament, medium polypeptide (NEFM; 1:500; Santa Cruz Biotechnology). Total protein loading and transfer onto the membranes were visualized by amidoblack staining.

Immunofluorescence microscopy

MIN6 cells were cultured on polylysine or laminin-coated coverslips for 2–5 d before staining. Cells were fixed in 4% paraformaldehyde for 10 min at room temperature, permeabilized with 0.2% Triton X-100 on ice for 10 min, blocked with 5% fetal calf serum for 30 min in PBS, and then incubated for 1 h with rabbit anti-ZBED6, guinea pig anti-insulin (Fitzgerald, Atlanta, GA, USA), rabbit anti-PDX1, mouse anti-NEFM, or tubulin β 3, class III (Tubb3) antibodies at room temperature. The cells were then washed 4 times with PBS to remove unbound antibodies and then treated with Alexa Fluor 488-labeled goat anti-rabbit and goat anti-mouse, Alexa Fluor 594-labeled goat anti-guinea pig, and goat anti-mouse secondary antibodies (20 μg/ml each; Thermo Fisher Scientific) for 1 h. Cells were washed 4 times with PBS, mounted with Vectashield Hard Set mounting medium with DAPI (Vector Laboratories, Burlingame, CA, USA), and inspected with a Nikon Eclipse C1/TE2000U microscope (Nikon).

Statistical analysis

Data are presented as means ± SEM. Statistical significance for pairwise comparisons was analyzed using Student's t test. One-way

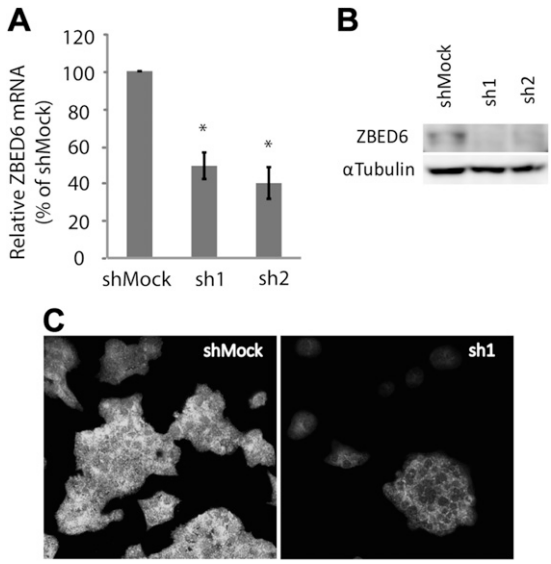

Figure 1. Validation of stable *Zbed6* silencing. MIN6 cells were transduced with either Zbed6 (sh1 or sh2) or mock (shMock) shRNA lentiviral vectors. *A*) Mean ± SEM from 3 qPCR measurements of *Zbed6* mRNA levels. $*P < 0.05$. *B*) Western blot of ZBED6 protein levels compared with α-tubulin staining. *C*) ZBED6 localization and the knockdown effect were investigated by immunofluorescence staining.

w.fasebj.org by The University of British Columbia Library (142.103.160.110) on July 28, 2018. The FASEB Journal Vol. ${article.issue.getVolume()}, No. ${article.issue.getIssueNum

ANOVA on ranks, followed by the Student-Newman-Keul method, was used for multiple comparisons. For identification of DE genes, we used an FDR value smaller than 0.05 and no cutoff limit. The FDR value is the multiple test-adjusted *P* value from the Student's *t* test based on the reads per kilobase per million mapped reads (RPKM) value for each of the 3 biologic replicates. Statistical significance is detailed in figure legends.

RESULTS

Stable *Zbed6* silencing in MIN6 cells

Lentiviral vectors that express 2 different *Zbed6*-specific shRNAs (sh1 and sh2) were used for stable silencing of *Zbed6* in the MIN6 cell line. We recently observed that the effects of sh1- and sh2-mediated *Zbed6* knockdown could be reversed by reconstitution of *Zbed6* expression, which strongly indicates that the sh1/sh2-induced phenotype occurs *via* specific *Zbed6* knockdown (9). A mock lentiviral vector containing a scrambled shRNA sequence was used to generate a negative control cell line (shMock). *Zbed6* silencing was confirmed by qPCR and a >50% reduction of *Zbed6* mRNA was achieved in the stable sh1 and sh2 cell lines (**Fig. 1*A***). Western blotting confirmed efficient suppression of ZBED6 protein expression in both cell lines (Fig. 1*B*). Immunofluorescence staining showed weak nuclear and strong cytoplasmic staining of ZBED6 in shMock MIN6 cells (Fig. 1*C*). In sh1 cells, both the nuclear and cytoplasmic staining of ZBED6 was dramatically decreased (Fig. 1*C*).

We also attempted to downregulate ZBED6 in human islet cells but failed as lentivirus-transduced islet cells exhibited low viability (results not shown).

ChIP-seq analysis with anti-ZBED6 antibody in MIN6 cells

We obtained 10 million uniquely aligned reads from 2 ChIP-seq libraries with high enrichment for ZBED6 in MIN6 cells (**Fig. 2*A***). Peak calling with model-based analysis of ChIP-seq (17) gave close to 30,000 peaks, and peaks of all heights were found to be enriched for the ZBED6 consensus-binding sequence GCTCG but at low levels among lower peaks (Fig. 2*B*). We thus increased the cutoff to a peak height of 30 to reduce the number of false-positive peaks, thereby limiting the list of significant peaks to 4070 (Supplemental Table S2). In agreement with our previous results from mouse C2C12 myoblast cells (1) and human islet cells (9), there was a preference for ZBED6-binding immediate downstream of transcription start sites (TSS; Fig. 2*C*), with a high overlap between peaks from the 2 mouse cell lines. The overlap between putative-binding sites in MIN6 islet cells and

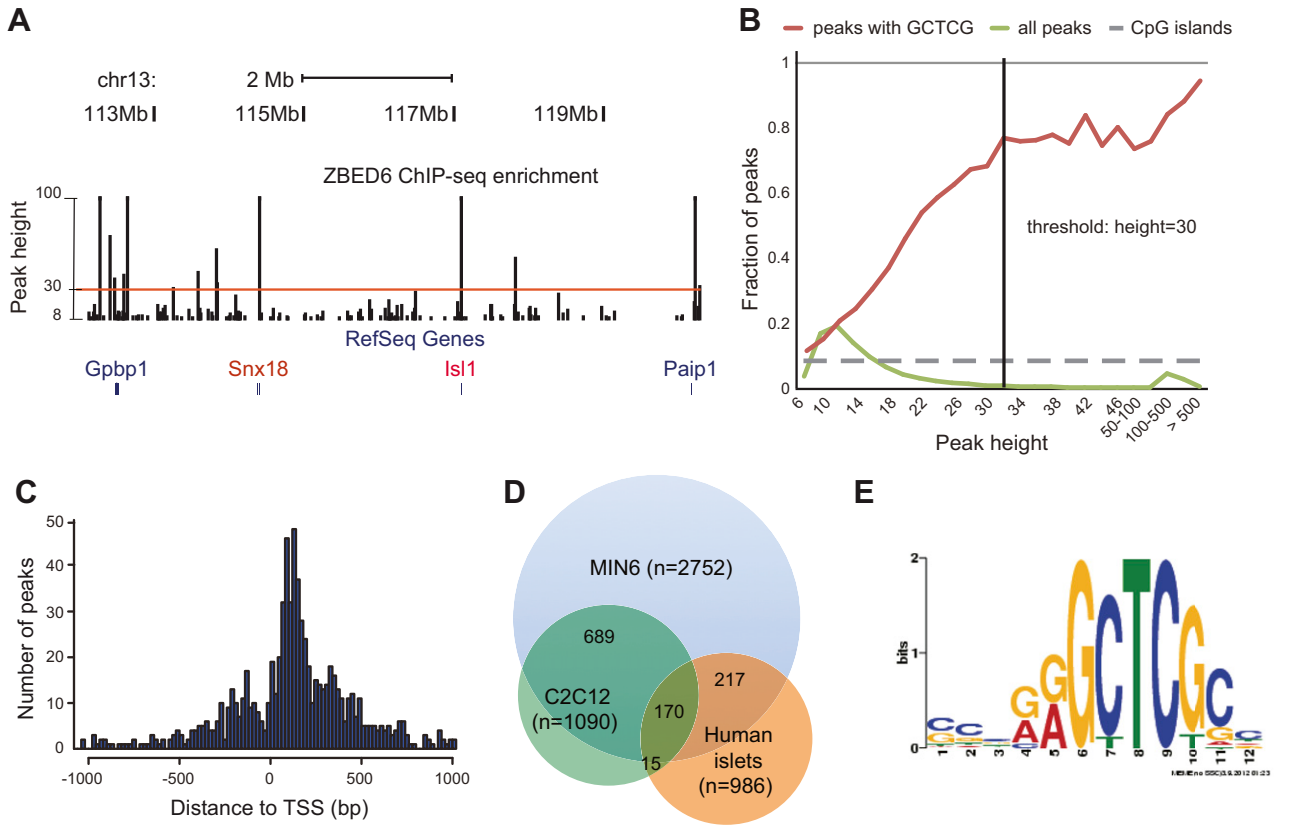

Figure 2. ChIP-seq analysis. *A*) ChIP-seq enrichment over a region on chr13 harboring the ISL1 transcription factor, LIM/homeodomain (*Isl1*) gene. The horizontal line indicates the cutoff used; *y*-axis is limited to 100 reads. The 4 RefSeq genes associated with the highest peaks are displayed, with upregulated genes in red. *B*) Fraction of peaks that has a match to GCTCG as a function of peak height (red) compared with that of negative regions (CpG islands; gray), with distribution of peak heights in green. *C*) Distribution of peaks around TSS. *D*) Overlaps of genes with a ZBED6 peak within 1 kb of TSS in mouse MIN6 and C2C12 myoblast cells compared with human islet cells. *E*) The top MEME-ChIP motif for ZBED6.

w.fasebj.org by The University of British Columbia Library (142.103.160.110) on July 28, 2018. The FASEB Journal Vol. ${article.issue.getVolume()}, No. ${article.issue.getIssueNum

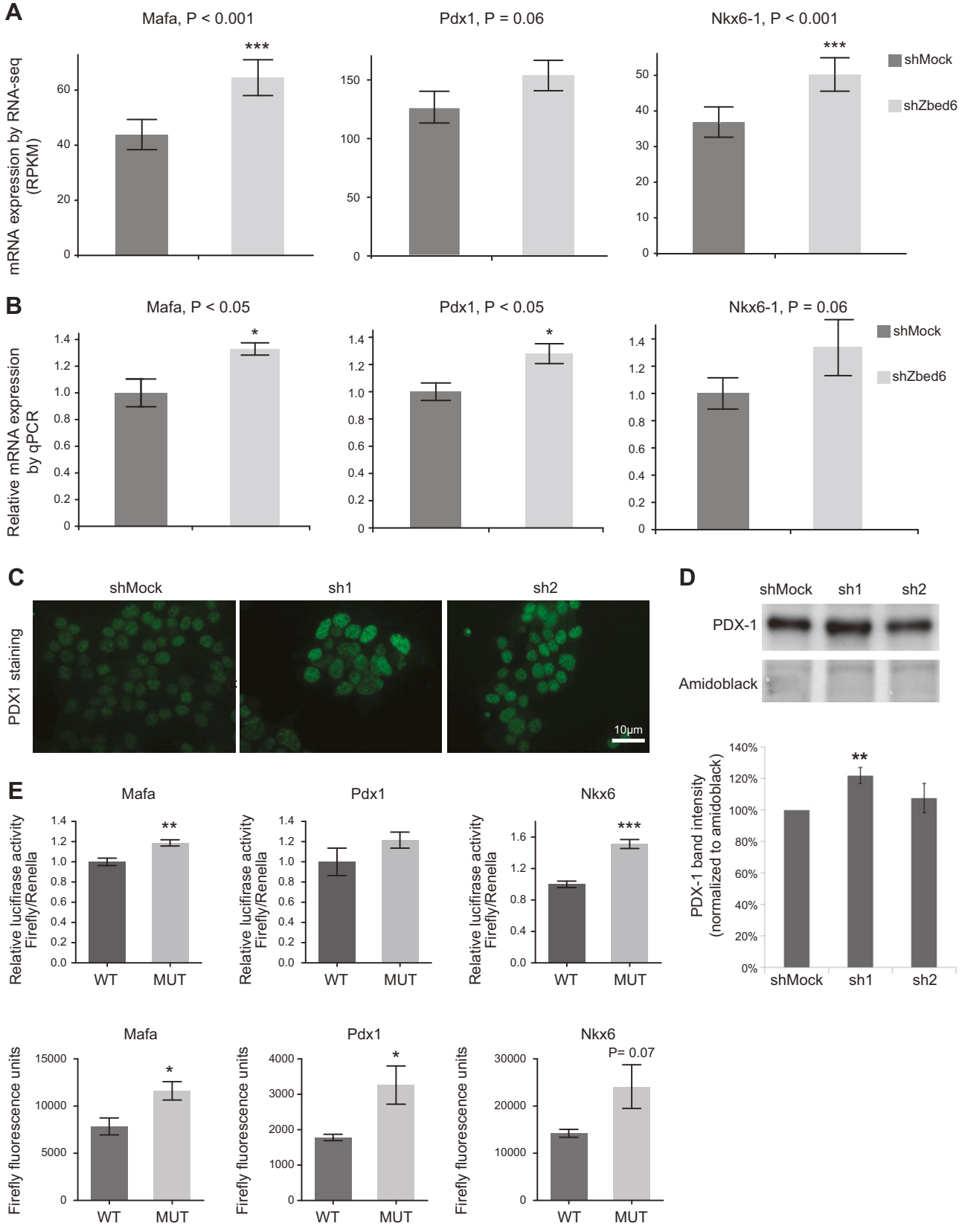

Figure 3. *Zbed6* knockdown enhanced expression of β-cell-specific transcription factors. *A–D*) RNA sequencing (*A*) and qPCR (*B*) results for *Mafa*, *Pdx1*, and *Nkx6-1* in shMock *vs.* sh1 *Zbed6*-silenced cells. The increased protein expression of Pdx1 was verified by immunofluorescence staining in both sh1 and sh2 *Zbed6*-silenced cells (*C*) and Western blotting (*D*). *E*) Firefly and *Renilla* luciferase activity was determined using *Mafa*, *Pdx1*, and *Nkx6-1* promoter constructs with or without mutations in ZBED6-binding sites. Results are means ± SEM for biologic triplicates (*A*, *B*) or 3–6 independent experiments (*C–E*). $^*P < 0.05$, $^{**}P < 0.01$, $^{***}P < 0.001$ using Student's paired *t* test.

w.fasebj.org by The University of British Columbia Library (142.103.160.110) on July 28, 2018. The FASEB Journal Vol. ${article.issue.getVolume()}, No. ${article.issue.getIssueNum

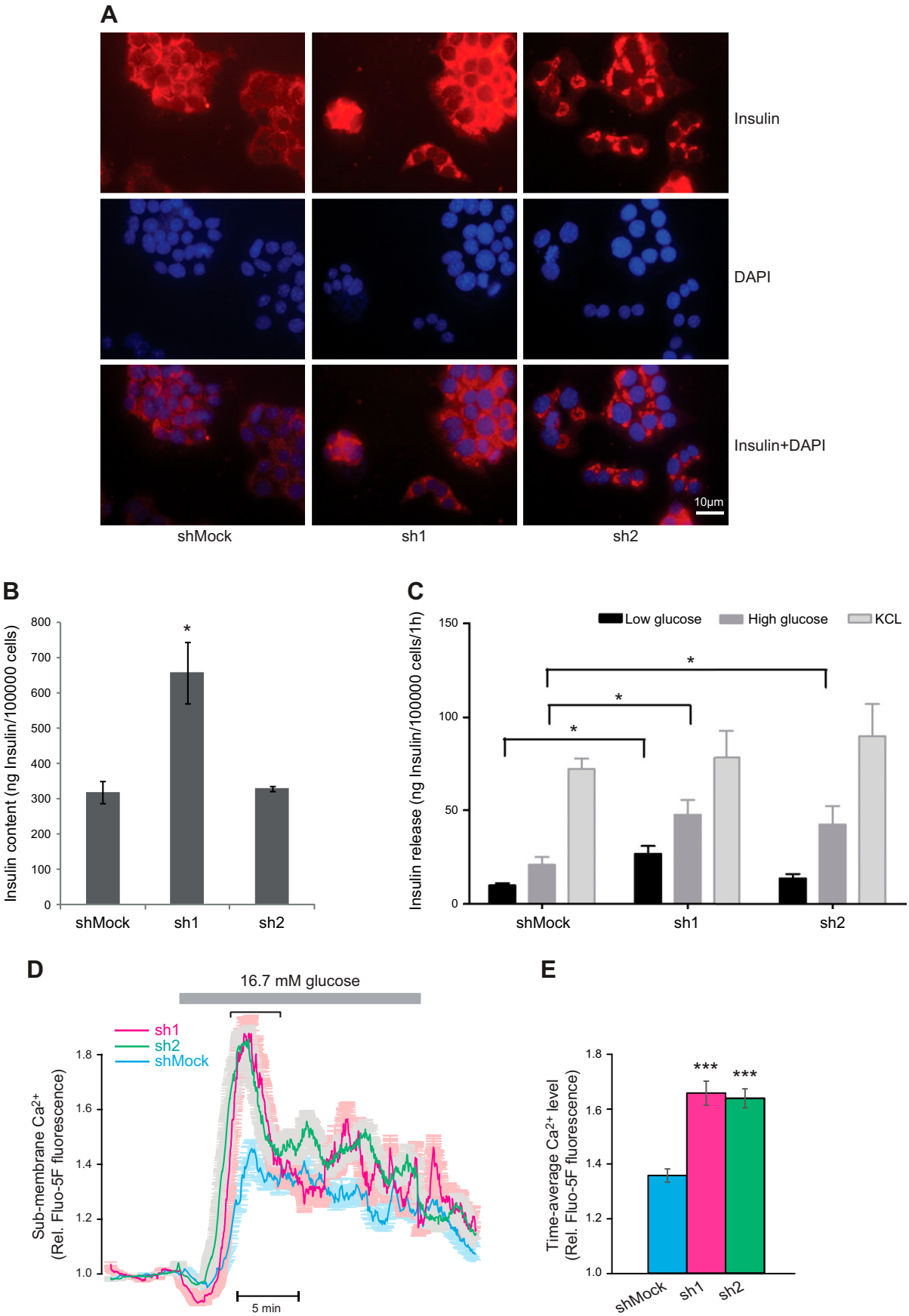

Figure 4. β-Cells with *Zbed6* knockdown contain and release more insulin. *A*) shMock, sh1, and sh2 MIN6 cells were stained with insulin (red) and DAPI (blue) after 5 d culture. Pictures were taken with a 63× oil objective. *B–C*) The insulin content (*B*) and insulin release (*C*)

(*continued on next page*)

w.fasebj.org by The University of British Columbia Library (142.103.160.110) on July 28, 2018. The FASEB Journal Vol. ${article.issue.getVolume()}, No. ${article.issue.getIssueNum

human islets was lower (39%) but increased with a more stringent cutoff in the human islet dataset to ~50%, indicating that many of the strong binding sites are evolutionary conserved between mouse and human but that the overlap is higher between cell types within species (Fig. 2*D* and Supplemental Table S2). The highest scoring motif identified using MEME-ChIP (11) was a 12 bp motif with a core GCTCG sequence (Fig. 2*E*), consistent with the previously established consensus motif for ZBED6 (1). This motif was present in 82.4% of the peaks, which shows that most of the identified peaks are at locations of direct ZBED6 binding. The ZBED6-binding genes that were in common for MIN6, C2C12, and human islet cells (Supplemental Table S3) were submitted for enrichment analysis of GO terms and Kyoto Encyclopedia of Genes and Genomes pathways using DAVID. We observed that 38 genes belonging the GO category "Transcription Regulation" (enrichment score 5.47) were significantly clustered ($P < 0.001$ using the Benjamini test), and among them were transcription factor coding genes *Nkx6-1*, *Maf*, CCAAT/enhancer binding protein α, sex-determining region Y-box 9, forkhead box o3, and WW domain containing adaptor with coiled-coil (Supplemental Table S4). No other GO categories were significantly clustered, suggesting that ZBED6 acts primarily as a transcriptional regulator.

Whole transcriptome analysis by mRNA sequencing

We generated 29–97 million 100 bp paired-end reads from triplicate sh1 and shMock samples, and 78–88% of these were uniquely mapped to the mouse genome using TopHat. We used Cufflinks with the RefSeq gene model to calculate the RPKM values and to identify DE genes. The shZBED6 and shMock samples showed a similar overall distribution of gene expression, with the majority of the genes expressed at a level in the range of 1–100 RPKM (Supplemental Fig. S1*A*). We detected 12,352 out of 24,468 (50.5%) annotated RefSeq with sufficient expression for DE analysis. Four genes that code for typical β-cell proteins (Insulin II, Islet amyloid polypeptide, Insulin like growth factor 2, and Secretogranin II) were all expressed at very high levels (Supplemental Fig. S1*B*). The genes for these 4 proteins had RPKM values above 2000 and contributed 6.8% of all mapped reads.

ZBED6 knockdown increases β-cell transcription factor expression, insulin content, and glucose-induced insulin release

We identified >700 DE genes with an FDR smaller than 5% after *Zbed6* silencing in MIN6 cells (Supplemental Table S5). The transcription factor genes *Mafa* and *Nkx6-1*, which are crucial for pancreatic β-cell maturation and function, were among the significantly upregulated genes (**Fig. 3*A, B***). *Pdx1*, another transcription factor of crucial importance in β-cells, also showed a trend of increased expression after *Zbed6* silencing (Fig. 3*A*), supported by qPCR (Fig. 3*B*). Interestingly, all 3 genes had ZBED6 peaks at the TSS, with peak heights for *Pdx1* and *Nkx6-1* well above the cutoff (Supplemental Table S2), indicating that they are repressed by ZBED6 at the transcriptional level. Immunostaining indicated increased PDX1 levels in the nuclei of sh1 and sh2 cells (Fig. 3*C*), and Western blotting showed a 22% increase (<0.01) of the PDX1 protein in sh1 cells (Fig. 3*D*). A trend to increased Pdx1 was observed in sh2 cells, but it did not reach statistical significance (Fig. 3*D*). Further support for direct ZBED6-mediated transcriptional control of *Pdx1*, *Mafa*, and *Nkx6-1* genes was obtained by luciferase reporter analysis. We observed that promoter constructs for these 3 genes, in which ZBED6-binding sites were mutated, generated stronger firefly luciferase signals compared with WT promoters (Fig. 3*E*). When expressing the *Firefly* signal as a ratio to the *Renilla* luciferase signal, both *Mafa* and *Nkx6-1* promoter-driven signals were significantly increased by the ZBED6-binding mutation, whereas the increase in *Pdx1* was borderline significant (Fig. 3*E*).

As the upregulation of *Mafa*, *Pdx1*, and *Nkx6-1* is compatible with a more mature β-cell phenotype, we also analyzed the content and release of insulin in these cells. Immunostaining of insulin indicated increased accumulation of insulin granules in the cytoplasm of most of the sh1 cells and some of the sh2 cells (**Fig. 4*A***). The insulin content was significantly higher in sh1 MIN6 compared with mock cells (Fig. 4*B*). The insulin release of both sh1 and sh2 MIN6 cells at a high-glucose concentration was significantly higher than in mock cells (Fig. 4*C*). In addition, an increase of insulin release at a low-glucose concentration was observed in sh1 cells, possibly reflecting the higher insulin content of these cells. The release of insulin in response to potassium chloride was not significantly different in sh1/sh2 cells compared with mock cells (Fig. 4*C*), indicating that depolarization-mediated insulin release is not affected by silencing of *Zbed6*. The increased glucose-stimulated insulin secretion in the ZBED6 knockdown cells was accompanied by a more pronounced glucose-induced rise of the cytoplasmic Ca^{2+} concentration in the subplasma membrane space, as evaluated with total internal reflection microscopy and the fluorescent Ca^{2+} indicator Fluo-5F (Fig. 4*D*). The differences between control and sh1 and sh2 cells were most pronounced during the initial 5 min when the time-averaged response was twice as high in the knockdown cells compared with control (Fig. 4*E*), but the Ca^{2+} levels were consistently higher in the knockdown cells throughout the stimulation period (Fig. 4*D*).

induced by 1.67 mM glucose (low), 16.7 mM glucose (high), and 30 mM KCl combined with 1.67 mM glucose were measured in shMock, sh1, and sh2 MIN6 cells. Results in *B* are means ± SEM for 4 independent experiments. $*P < 0.05$, Student's *t* test. Results in *C* are means ± SEM for 6 independent experiments, $*P < 0.05$ using 1-way ANOVA on ranks followed by the Student-Newman-Keul test. *D*) Subplasma membrane Ca^{2+} recordings from shMock, sh1, and sh2 MIN6 cells during elevation of the glucose concentration from 1.67 to 16.7 mM. Means ± SEM of Fluo-5F fluorescence recorded with total internal reflection microscopy from 213 (shMock), 131 (sh1), and 173 (sh2) cells from 3 independent experiments. *E*) Means ± SEM for the time-average Ca^{2+} level during the initial increase, indicated by a bracket in *D*. $***P < 0.001$ for difference from shMock, Student's *t* test.

w.fasebj.org by The University of British Columbia Library (142.103.160.110) on July 28, 2018. The FASEB Journal Vol. ${article.issue.getVolume()}, No. ${article.issue.getIssueNum

Zbed6 knockdown enhanced cAMP content in response to forskolin and IBMX

Apart from the triggering role of Ca^{2+}, accumulating evidence indicates that glucose-induced insulin secretion is markedly amplified by cAMP. cAMP is synthesized from ATP by adenylyl cyclases (ACs) and degraded by phosphodiesterases (PDE). Interestingly, our RNA sequencing results showed that zbed6 knockdown resulted in increased levels of mRNA coding for ACs Adcy1 and Adcy9 and decreased levels for PDEs Pde3a/5a/6a/8a/10a (**Table 1**). When stimulated with forskolin, an enhanced cAMP content was observed in sh1 cells (**Fig. 5**).

Genes associated with neuronal differentiation and cell adhesion were significantly over-represented among DE genes after *Zbed6* silencing

Having observed that ZBED6 antagonizes the mature β-cell phenotype, we submitted all DE genes for enrichment analysis of GO terms and Kyoto Encyclopedia of Genes and Genomes pathways using DAVID analysis to study whether other aspects of β-cell function were affected by ZBED6. Several GO categories were significantly enriched (FDR-corrected $P < 0.05$), including neuronal differentiation and projection, cell projection, regulation of neuronal differentiation, generation of precursor metabolites, axon guidance molecules, MAPK signaling pathway, and cell adhesion (**Fig. 6*A***). Among these, we decided to focus on cell adhesion and neuronal differentiation, 2 important processes involved in β-cell maturation and function (18–20). Therefore, 18 out of ~70 DE genes that belong to the 2 categories—neuronal differentiation and cell adhesion—were randomly selected for qPCR validation, 10 from the first category (Sonic hedgehog (Shh), Semaphorin 6a (Sema6a), *Nkx6*-1, Neurofilament, light polypeptide (Nelf), LIM homeobox protein 2 (Lhx2), *Isl1*, Dihydropyrimidinase-like 5 (Dpysl5), CD24a antigen (Cd24a), BR serine/threonine kinase 2 (Brsk2), and Activated leukocyte cell adhesion molecule (Alcam)) and the remaining 8 from the second category [Transmembrane protein 8 (five membrane-spanning domains) (Tmem8), protocadherin 19 (Pcdh19) Neuropilin 2 (Nrp2), Nephronectin (Npnt), Immunoglobulin superfamily, member 11 (Igsf11), Catenin delta 2 (Ctnnd2), cadherin 23 (Cdh23) and Brevican (Bcan)]. All genes except 1 showed the same direction of expression changes in both RNA sequencing and qPCR analysis and one-half of them was also significantly affected in the qPCR analysis (Fig. 6*B*). Thus, ZBED6 affects the expression of genes that control neuronal differentiation and cell adhesion.

TABLE 1. *Zbed6 knockdown affects expression of ACs and PDEs*

Gene	shMock	shZbed6	log2 (fold change of shZbed6 to shMock)	*P*
Adcy9	15.1754	20.3737	0.424974	5.92E-05
Adcy1	2.24748	6.11523	1.4441	0.00114
Pde6a	2.65377	1.69154	−0.649701	0.00116
Pde5a	1.28682	0.787112	−0.709171	0.00135
Pde10a	7.77087	6.0643	−0.357735	0.00171
Pde8a	12.5159	9.43184	−0.408149	0.00243
Pde3a	1.29783	0.648056	−1.00191	0.00044

The mRNA expression of ACs and PDEs was measured by RNA sequencing in shMock and sh1 Zbed6-silenced cells. The average mRNA expression levels (RPKM) of triplicates of shMock and sh1 MIN6 cells were listed in the table.

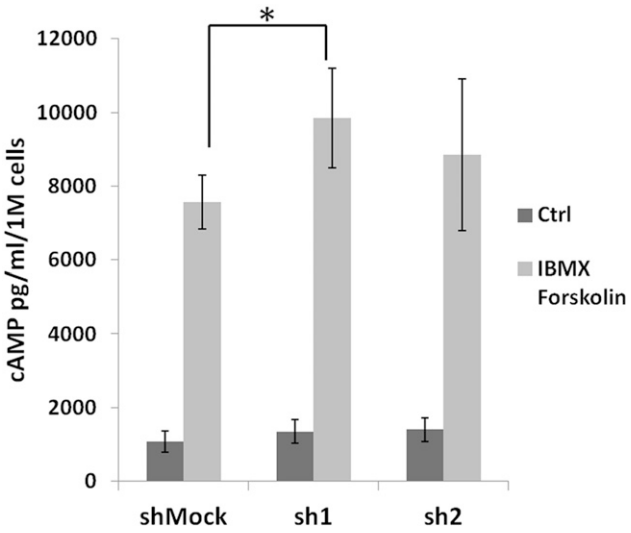

Figure 5. Zbed6 knockdown enhanced cAMP content in response to forskolin and IBMX. cAMP was measured at basal conditions (control) and after stimulation with 10 μM forskolin and 100 μM IBMX for 20 min using a commercial ELISA kit (Cayman Chemical). The results were normalized to the cell number (per 1 million cells) in each well. Nine replicates were measured, and data are presented as means ± SEM. *$P \pm 0.05$, Student's *t* test.

Genes with ZBED6-binding sites are overrepresented among DE genes

We overlapped the list of ChIP-seq peaks with the DE genes (Supplemental Tables S2 and S6) and identified 239 (32.7%) DE genes with at least 1 ZBED6 site within 10 kb up- or downstream of the TSS (Supplemental Table S6), compared with binding at 24.3% of expressed non-DE genes. Thus, there is a statistically significant over-representation of genes with ZBED6-binding sites among DE genes ($P < 0.0001$) after stable silencing of *Zbed6* (**Table 2**). The DE genes with ZBED6 binding were also enriched for several GO terms including "regulation of neuronal differentiation" and "cell adhesion" (Fig. 6*C*). Among the 10 DE genes associated with regulation of neuronal differentiation, Semaphorin 6a, *Nkx6-1*, Neurophilament, light polypeptide, LIM homeobox protein 2, *Isl1*, Dihydropyridiminase-like 5, and BR serine/threonine kinase 2 were all upregulated after stable *Zbed6* silencing, whereas 3 genes (Sonic hedgehog, CD24 antigen, and Activated lymphocyte cell adhesion molecule) were downregulated, as assessed by RNA sequencing and qPCR (Fig. 6*B*).

Zbed6 knockdown affects cell morphology/growth patterns and promotes the formation of NEFM-positive and axon-like protrusions

Having observed that *Zbed6* silencing causes alterations in the expression of genes involved in neuronal differentiation

w.fasebj.org by The University of British Columbia Library (142.103.160.110) on July 28, 2018. The FASEB Journal Vol. ${article.issue.getVolume()}, No. ${article.issue.getIssueNum

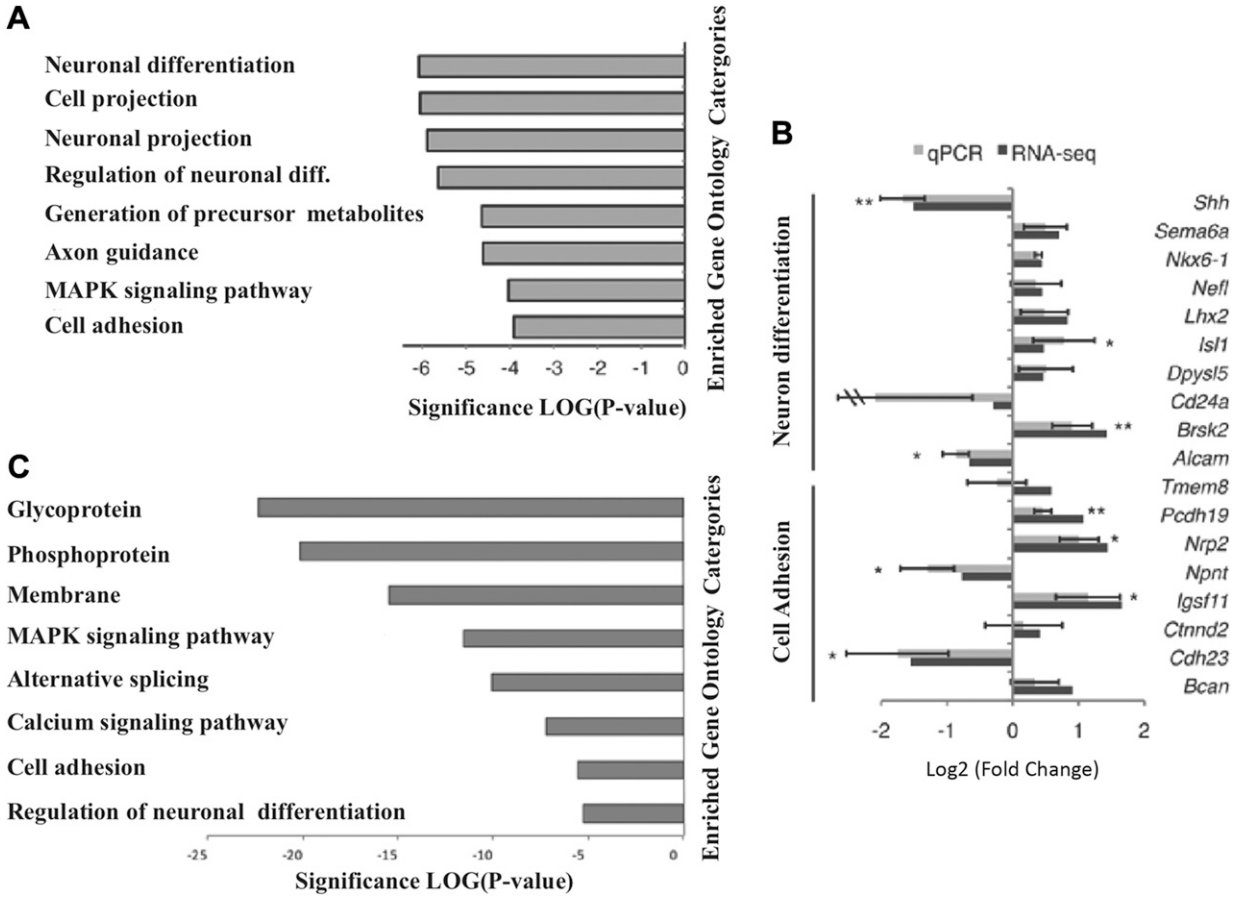

Figure 6. Genes associated with neuronal differentiation and cell adhesion were over-represented among DE genes after *Zbed6* silencing. *A*) The significantly enriched GO categories (*y*-axis) among the 731 DE genes with an FDR < 0.05. *B*) The log2 fold changes detected by RNA sequencing and qPCR of the DE genes associated with neuronal differentiation and cell adhesion. *C*) Significantly enriched GO categories (*y*-axis) among the DE genes that had at least 1 ZBED6-binding site within 10 kb, up- or downstream of the TSS.

and cell adhesion, we next analyzed cell morphology during culture with or without laminin coating. Interestingly, clear morphologic differences were observed after a 5 d culture period in the absence of laminin coating when comparing sh1 and sh2 cells with mock-transfected cells. The sh1 and sh2 cells were more aggregated and formed 3-dimensional structures, whereas the control cells, to a higher extent, spread out as a traditional monolayer (**Fig. 7*A***). This indicates that ZBED6 is required for monolayer growth on a plastic support. As laminin is a crucial component of the non-transformed β-cell extracellular matrix, we next investigated the effects of knockdown of *Zbed6* on MIN6 cells morphology cultured on a laminin-coated support. In this case, the 3-dimensional cell clusters were still evident in the sh1 and sh2 cell lines after 5 d of culture. In addition, thin and extended axon-like protrusions were observed to originate from the *Zbed6*-silenced cells (Fig. 7*A*). Based on the enrichment of genes associated to the neuronal differentiation category among the DE genes and that ZBED6 binds to the upregulated *Nefm* gene, we analyzed NEFM immunoreactivity in the different MIN6 cell lines. shMock cells were only weakly stained for NEFM, with some cells showing no NEFM immunoreactivity at all, whereas sh1 and sh2 cells exhibited clear NEFM staining (Fig. 7*B*). We observed in sh1/sh2 MIN6 cells dense NEFM fibers present in the axon-like protrusions (Fig. 7*B*). The increased expression of NEFM in sh1 and sh2 cells was also confirmed by Western blotting (Fig. 7*C*). Finally, we also stained for Tubb3, which is also a neurodifferentiation marker, and in this case, we observed increased cytoplasmic staining in sh1 and sh2 cells compared with the mock-transfected cells (Fig. 7*B*).

DISCUSSION

Our previous studies have demonstrated that a mutation abolishing 1 single ZBED6 site in *IGF2* has a major effect on muscle growth and alters the body composition of pigs and that ZBED6 controls insulin production, proliferation, and apoptosis of β-TC6 cells (1, 9). The present study

TABLE 2. *Analysis of the correlation between DE after stable Zbed6 silencing in MIN6 cells and the presence of ZBED6-binding sites within 10 kb of the TSS of expressed genes*

ZBED6 sites	DE genes	Non-DE genes
Yes	239 (32.7%)[a]	3002 (24.3%)
No	492 (67.3%)	9350 (75.7%)
Total	731	12,352

[a]Over-representation of genes with ZBED6-binding sites among DE genes (χ^2 test, 2-tailed, $P < 0.0001$).

w.fasebj.org by The University of British Columbia Library (142.103.160.110) on July 28, 2018. The FASEB Journal Vol. ${article.issue.getVolume()}, No. ${article.issue.getIssueNum

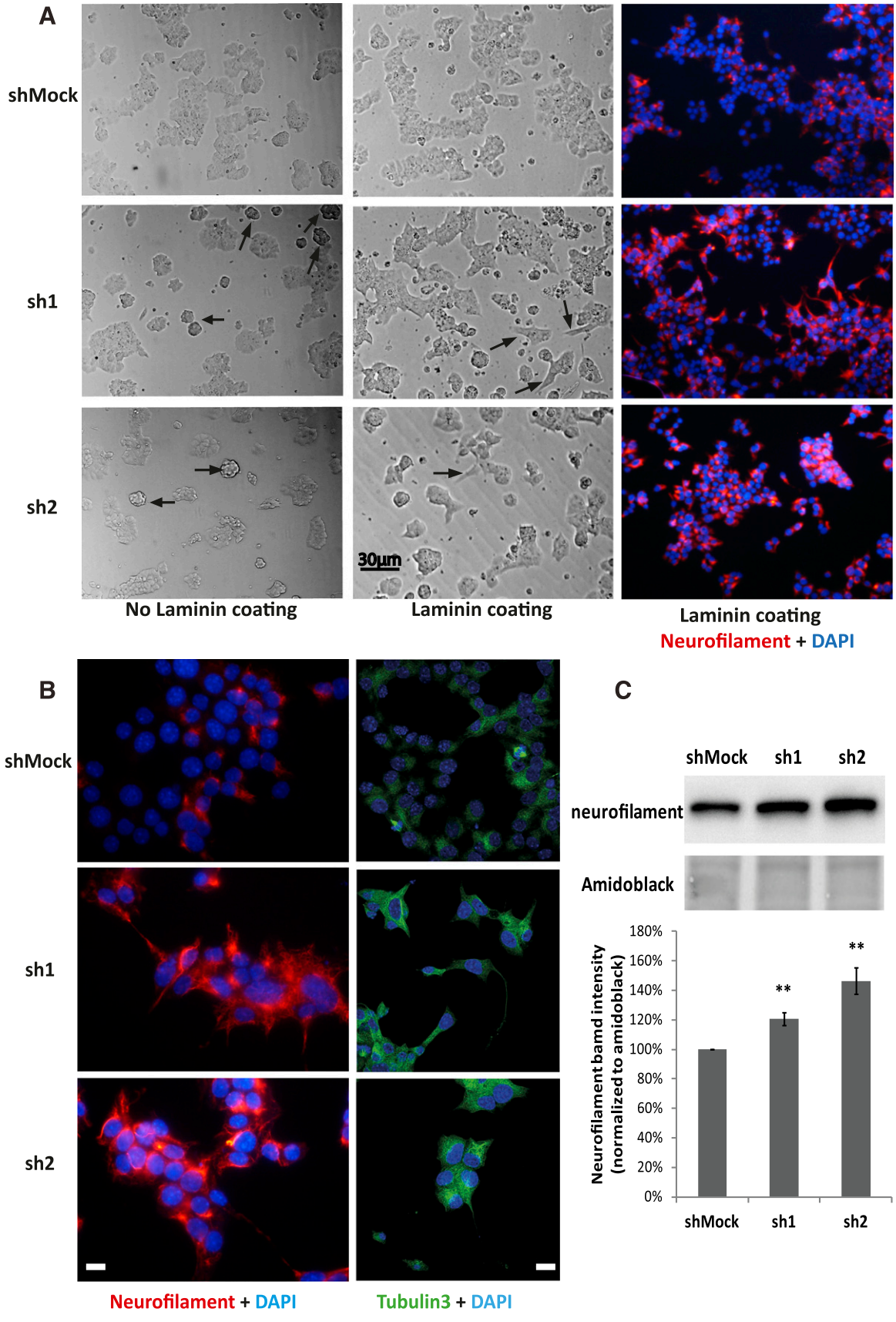

Figure 7. *Zbed6* knockdown affected cell morphology and upregulated NEFM and Tubb3 expression. *A*) Morphology of shMock, sh1, and sh2 MIN6 cells after 5 d of culture with or without laminin; equal numbers of cells were seeded to Nunc plastic culture plates with or without 10 μg/ml laminin coating. Arrowheads (no laminin coating; left) point to cell aggregates; arrowheads (laminin coating; middle) point to axon-like protrusions. *B*) Staining of NEFM and Tubb3 in shMock, sh1, and sh2 MIN6 cells on

(*continued on next page*)

w.fasebj.org by The University of British Columbia Library (142.103.160.110) on July 28, 2018. The FASEB Journal Vol. ${article.issue.getVolume()}, No. ${article.issue.getIssueNum

confirms and extends the findings from β-TC6 cells, as our ChIP-seq and RNA sequencing results strongly suggest that ZBED6 is an important transcriptional regulator in the insulin-producing MIN6 cell line. We observed >700 DE genes and an enrichment for ZBED6-binding sites among upregulated genes in *Zbed6*-silenced cells. Among the genes with higher expression in *Zbed6*-silenced cells were *Pdx1*, *Mafa*, and *Nkx6-1*. Mutation of ZBED6-binding sites in these gene promoters resulted in increased reporter gene activities, indicating direct gene promoter binding leading to suppression of transcription. PDX1 is known to play a key role in both pancreatic lineage determination and β-cell terminal differentiation (21), and it also promotes insulin gene transcription in mature β-cells by binding to the insulin promoter (22). The transcription factor MAFA cooperates with PDX1 in the activation of insulin transcription and in the stimulation of terminal β-cell differentiation (23). NKX6-1 is required for the development of β-cell precursors during the second wave of β-cell development (24). Therefore, it is highly noteworthy that the expression of these 3 important β-cell transcription factors was coordinatively suppressed by ZBED6 and that strong ZBED6 binding was found for both the *Pdx1* and *Nkx6*-1 genes.

In addition to the well-known β-cell transcription factors MAFA, PDX1, and NKX6-1, we observed ZBED6 binding to some 35 other transcription-related genes that were common targets for ZBED6 among the 3 different cell types MIN6, C2C12, and human islet cells. Among these genes was, for example, CCAAT/enhancer binding protein α, a transcription factor primarily involved in hematopoietic cell differentiation but also expressed in β-cells, where it seems to mediate proapoptotic effects in response to proinflammatory cytokines (25). A second ZBED6-binding gene of putative importance was sex-determining region Y-box 9, a regulator of early embryonic duodenal and pancreatic differentiation (26). Thirdly, ZBED6 may target WW domain containing adaptor with coiled-coil, a gene that seems to be induced during differentiation of induced pluripotent stem cells to immature β-cells (27). These examples of putative ZBED6 – target gene interactions may indicate an anti-differentiation/apoptosis effect of ZBED6, but further experimentation will be necessary to verify such specific roles of ZBED6.

In further support of ZBED6 acting as an anti-β-cell maturation factor, we observed that MIN6 cells with lowered ZBED6 expression contained more insulin and released more insulin at a high-glucose concentration. Thus, the role of ZBED6 may be to maintain proliferation and prevent premature β-cell differentiation during different precursor stages preceding the terminally differentiated and nonreplicating β-cell. This fits well with our recent finding that *Zbed6* knockdown in insulin-producing β-TC6 cells resulted in a restricted proliferation and an enhanced insulin production (9) and that *Zbed6* silencing in mouse C2C12 myoblasts promotes differentiation and the formation of myotubes (1). Clearly, further studies on ZBED6 expression and function during normal and pathologic β-cell differentiation/regeneration are warranted.

A mature β-cell requires not only insulin gene expression but also the activation of specific gene networks that mediate proper hormone secretion and cell adhesion. It is well known that β-cells resemble neurons, as both cell types are excitable and capable of regulated secretion. Martens *et al.* (19) reported that 15% of conserved β-cell markers were shared with neurons and that these genes were mainly involved in regulating synaptic vesicle transport. It has also been observed that a MIN6 subline with an intact glucose-induced insulin release expressed more NEFM and Nefl than a MIN6 subline with an impaired insulin release (28) and that a small molecule neuronal differentiation inducer increased insulin expression and release in MIN6 cells (20). Thus, it is likely that increased β-cell neuronal differentiation underlies an improved insulin release and β-cell function. In the present investigation, *Zbed6* silencing resulted mainly in upregulation of genes belonging to the GO category neuronal differentiation. A characteristic feature of both neurons and β-cells is that exocytosis is triggered by voltage-dependent Ca^{2+} influx. The more pronounced glucose-induced Ca^{2+} increases after Zbed6 silencing provide a direct explanation to the enhanced insulin secretion at high-glucose concentrations. Ca^{2+}-triggered insulin secretion can be amplified by cAMP. Increased levels of ACs AC1 and AC9, as well as decreased levels of PDEs PDE3a/5a/6a/8a/10a in zbed6-silenced cells indicate a higher cAMP synthesis capacity upon stimulation in this type of cells. Indeed, when triggered by forskolin, an enhanced cAMP content has been observed in zbed6-silenced cells. We therefore suggest that increased cAMP levels may contribute to the enhanced glucose-induced insulin secretion in zbed6-silenced cells. An anti-neuronal differentiation function of ZBED6 is further supported by our observations that *Zbed6*-silenced β-cells formed pointed and axon-like protrusions, which stained for NEFM, and that also Nelf and microtubule-associated protein τ were upregulated in *Zbed6*-silenced cells. Interestingly, not only do mouse MIN6 cells respond to increased neuronal differentiation with improved β-cell function, but also, rat RINm5F cells have been reported to release more insulin when neuronally differentiated in response to nerve growth factor (29, 30).

Zbed6 silencing also led to upregulation of the majority of DE cell adhesion genes. These included Cdh4, a classic Cdh that is preferentially expressed in β-cells and neuronal cells (31) and forms adherens junctions during mesenchymal to epithelial transitions (32), and Pcdh (*Pcdh17* and *Pcdh19*), which seem to mediate homotypic cell-to-cell binding (33), suggesting increased epithelial cell–cell adhesion in the *Zbed6*-silenced MIN6 cells. Interestingly, *cdh23*, which seems to mediate heterotypic cell-to-cell adhesion (34), was decreased in ZBED6-deficient cells. These results are consistent with the increased formation of islet-like cell clusters that we

laminin-coated coverslips. Equal numbers of cells were cultured on 10 μg/ml laminin-coated coverslips for 5 d and then stained with anti-NEFM (red) and Tubb3 (green) antibodies. DAPI is blue. Pictures were taken with 63× objective. *C*) The increased protein expression of NEFM after *Zbed6* silencing was verified by Western blotting. Equal numbers of cells were seeded to standard 6-well culture plates without any coating and cultured for 5 d before analysis.

w.fasebj.org by The University of British Columbia Library (142.103.160.110) on July 28, 2018. The FASEB Journal Vol. ${article.issue.getVolume()}, No. ${article.issue.getIssueNum

observed in *Zbed6*-silenced cells (35). It is well established that intercellular interactions within islets of Langerhans are important for the development and maintenance of the β-cell phenotype, and this is associated with increased insulin expression and release (36). Accordingly, it has been reported that the function of MIN6 improves when the cells aggregate into 3-dimensional islet-like structures, known as pseudoislets (37). More recently, it has become increasingly clear that β-cells rely not only on the adhesion to other β-cells but more importantly, to basal membrane components derived from islet endothelial cells, a process that also requires expression of appropriate cell adhesion molecules (18). Furthermore, we have recently observed an increase in cell-to-cell contacts between *Zbed6*-silenced β-cells and neural crest stem cells (35). Thus, we propose that ZBED6 silencing modulates β-cell adhesion factor expression and that this contributes to improved function.

CONCLUSIONS

In summary, the results of this investigation indicate that ZBED6-mediated transcriptional regulation causes diminished β-cell adhesion, neuronal differentiation, and insulin production. It is easily envisaged that ZBED6 activity is required during early stages of β-cell differentiation to prevent premature or improper development. Today, many attempts are focused on the generation of new β-cells for transplantation or *in situ* regeneration purposes. In this context, it is possible that strategies aimed at increasing β-cell proliferation benefit from forced ZBED6 overexpression and that strategies aimed at stimulating β-cell maturation benefit from decreased ZBED6 expression. FJ

ACKNOWLEDGMENTS

Sequencing was performed by the SNP&SEQ Technology Platform, supported by Uppsala University and Hospital, SciLife Lab–Uppsala, and the Swedish Research Council (80576801 and 70374401). Computer resources were supplied by UPPMAX. This work was supported by the Swedish Research Council, Knut and Alice Wallenberg Foundation, Swedish Diabetes Association, Family Ernfors Fund, Barndiabetesfonden, EXODIAB, and Novo-Nordisk Foundation. L.J. was supported by Beijing Natural Science Foundation (6164040). The authors declare no conflicts of interest.

AUTHOR CONTRIBUTIONS

X. Wang, L. Jiang, O. Wallerman, S. Younis, Q. Yu, and A. Klaesson performed the experiments and analyzed the data; A. Tengholm, N. Welsh, and L. Andersson planned the study; and X. Wang, L. Jiang, O. Wallerman, and L. Andersson wrote the paper with input from all authors.

REFERENCES

1. Markljung, E., Jiang, L., Jaffe, J. D., Mikkelsen, T. S., Wallerman, O., Larhammar, M., Zhang, X., Wang, L., Saenz-Vash, V., Gnirke, A., Lindroth, A. M., Barrés, R., Yan, J., Strömberg, S., De, S., Pontén, F., Lander, E. S., Carr, S. A., Zierath, J. R., Kullander, K., Wadelius, C., Lindblad-Toh, K., Andersson, G., Hjälm, G., and Andersson, L. (2009) ZBED6, a novel transcription factor derived from a domesticated DNA transposon regulates IGF2 expression and muscle growth. *PLoS Biol.* **7**, e1000256
2. Andersson, L., Andersson, G., Hjälm, G., Jiang, L., Lindblad-Toh, K., Lindroth, A. M., Markljung, E., Nyström, A. M., Rubin, C. J., and Sundström, E. (2010) ZBED6: the birth of a new transcription factor in the common ancestor of placental mammals. *Transcription* **1**, 144–148
3. Van Laere, A. S., Nguyen, M., Braunschweig, M., Nezer, C., Collette, C., Moreau, L., Archibald, A. L., Haley, C. S., Buys, N., Tally, M., Andersson, G., Georges, M., and Andersson, L. (2003) A regulatory mutation in IGF2 causes a major QTL effect on muscle growth in the pig. *Nature* **425**, 832–836
4. Younis, S., Schönke, M., Massart, J., Hjortebjerg, R., Sundström, E., Gustafson, U., Björnholm, M., Krook, A., Frystyk, J., Zierath, J. R., and Andersson, L. (2018) The ZBED6-IGF2 axis has a major effect on growth of skeletal muscle and internal organs in placental mammals. *Proc. Natl. Acad. Sci. USA* **115**, E2048–E2057
5. Calderari, S., Gangnerau, M. N., Thibault, M., Meile, M. J., Kassis, N., Alvarez, C., Portha, B., and Serradas, P. (2007) Defective IGF2 and IGF1R protein production in embryonic pancreas precedes beta cell mass anomaly in the Goto-Kakizaki rat model of type 2 diabetes. *Diabetologia* **50**, 1463–1471
6. Casellas, A., Mallol, C., Salavert, A., Jimenez, V., Garcia, M., Agudo, J., Obach, M., Haurigot, V., Vilà, L., Molas, M., Lage, R., Morró, M., Casana, E., Ruberte, J., and Bosch, F. (2015) Insulin-like growth factor 2 overexpression induces β-cell dysfunction and increases beta-cell susceptibility to damage. *J. Biol. Chem.* **290**, 16772–16785
7. Devedjian, J. C., George, M., Casellas, A., Pujol, A., Visa, J., Pelegrín, M., Gros, L., and Bosch, F. (2000) Transgenic mice overexpressing insulin-like growth factor-II in beta cells develop type 2 diabetes. *J. Clin. Invest.* **105**, 731–740
8. Mercader, J. M., Liao, R. G., Bell, A. D., Dymek, Z., Estrada, K., Tukiainen, T., Huerta-Chagoya, A., Moreno-Macías, H., Jablonski, K. A., Hanson, R. L., Walford, G. A., Moran, I., Chen, L., Agarwala, V., Ordoñez-Sánchez, M. L., Rodríguez-Guillen, R., Rodríguez-Torres, M., Segura-Kato, Y., García-Ortiz, H., Centeno-Cruz, F., Barajas-Olmos, F., Caulkins, L., Puppala, S., Fontanillas, P., Williams, A. L., Bonàs-Guarch, S., Hartl, C., Ripke, S., Tooley, K., Lane, J., Zerrweck, C., Martínez-Hernández, A., Córdova, E. J., Mendoza-Caamal, E., Contreras-Cubas, C., González-Villalpando, M. E., Cruz-Bautista, I., Muñoz-Hernández, L., Gómez-Velasco, D., Alvirde, U., Henderson, B. E., Wilkens, L. R., Le Marchand, L., Arellano-Campos, O., Riba, L., Harden, M., Gabriel, S., Abboud, H. E., Cortes, M. L., Revilla-Monsalve, C., Islas-Andrade, S., Soberon, X., Curran, J. E., Jenkinson, C. P., DeFronzo, R. A., Lehman, D. M., Hanis, C. L., Bell, G. I., Boehnke, M., Blangero, J., Duggirala, R., Saxena, R., MacArthur, D., Ferrer, J., McCarroll, S. A., Torrents, D., Knowler, W. C., Baier, L. J., Burtt, N., González-Villalpando, C., Haiman, C. A., Aguilar-Salinas, C. A., Tusié-Luna, T., Flannick, J., Jacobs, S. B. R., Orozco, L., Altshuler, D., and Florez, J. C.; Diabetes Prevention Program Research Group, Broad Genomics Platform, T2D-GENES Consortium, SIGMA T2D Genetics Consortium. (2017) A loss-of-function splice acceptor variant in *IGF2* is protective for type 2 diabetes. *Diabetes* **66**, 2903–2914
9. Wang, X., Jiang, L., Wallerman, O., Engström, U., Ameur, A., Gupta, R. K., Qi, Y., Andersson, L., and Welsh, N. (2013) Transcription factor ZBED6 affects gene expression, proliferation, and cell death in pancreatic beta cells. *Proc. Natl. Acad. Sci. USA* **110**, 15997–16002
10. Li, H., Handsaker, B., Wysoker, A., Fennell, T., Ruan, J., Homer, N., Marth, G., Abecasis, G., and Durbin, R.; 1000 Genome Project Data Processing Subgroup. (2009) The sequence alignment/map format and SAMtools. *Bioinformatics* **25**, 2078–2079
11. Bailey, T. L., Boden, M., Buske, F. A., Frith, M., Grant, C. E., Clementi, L., Ren, J., Li, W. W., and Noble, W. S. (2009) MEME SUITE: tools for motif discovery and searching. *Nucleic Acids Res.* **37** (Web Server issue), W202–W208
12. Trapnell, C., Pachter, L., and Salzberg, S. L. (2009) TopHat: discovering splice junctions with RNA-Seq. *Bioinformatics* **25**, 1105–1111
13. Trapnell, C., Williams, B. A., Pertea, G., Mortazavi, A., Kwan, G., van Baren, M. J., Salzberg, S. L., Wold, B. J., and Pachter, L. (2010) Transcript assembly and quantification by RNA-Seq reveals unannotated transcripts and isoform switching during cell differentiation. *Nat. Biotechnol.* **28**, 511–515
14. Lizio, M., Harshbarger, J., Shimoji, H., Severin, J., Kasukawa, T., Sahin, S., Abugessaisa, I., Fukuda, S., Hori, F., Ishikawa-Kato, S., Mungall, C. J., Arner, E., Baillie, J. K., Bertin, N., Bono, H., de Hoon, M., Diehl, A. D., Dimont, E., Freeman, T. C., Fujieda, K., Hide, W., Kaliyaperumal, R.,

w.fasebj.org by The University of British Columbia Library (142.103.160.110) on July 28, 2018. The FASEB Journal Vol. ${article.issue.getVolume()}, No. ${article.issue.getIssueNum

Katayama, T., Lassmann, T., Meehan, T. F., Nishikata, K., Ono, H., Rehli, M., Sandelin, A., Schultes, E. A., 't Hoen, P. A., Tatum, Z., Thompson, M., Toyoda, T., Wright, D. W., Daub, C. O., Itoh, M., Carninci, P., Hayashizaki, Y., Forrest, A. R., and Kawaji, H.; FANTOM consortium. (2015) Gateways to the FANTOM5 promoter level mammalian expression atlas. *Genome Biol.* **16**, 22

15. Jiang, L., Wallerman, O., Younis, S., Rubin, C. J., Gilbert, E. R., Sundström, E., Ghazal, A., Zhang, X., Wang, L., Mikkelsen, T. S., Andersson, G., and Andersson, L. (2014) ZBED6 modulates the transcription of myogenic genes in mouse myoblast cells. *PLoS One* **9**, e94187
16. Idevall-Hagren, O., Jakobsson, I., Xu, Y., and Tengholm, A. (2013) Spatial control of Epac2 activity by cAMP and Ca2+-mediated activation of Ras in pancreatic β cells. *Sci. Signal.* **6**, ra29.1–ra29.11, S1–S6
17. Zhang, Y., Liu, T., Meyer, C. A., Eeckhoute, J., Johnson, D. S., Bernstein, B. E., Nusbaum, C., Myers, R. M., Brown, M., Li, W., and Liu, X. S. (2008) Model-based analysis of ChIP-Seq (MACS). *Genome Biol.* **9**, R137
18. Kragl, M., and Lammert, E. (2010) Basement membrane in pancreatic islet function. *Adv. Exp. Med. Biol.* **654**, 217–234
19. Martens, G. A., Jiang, L., Hellemans, K. H., Stangé, G., Heimberg, H., Nielsen, F. C., Sand, O., Van Helden, J., Van Lommel, L., Schuit, F., Gorus, F. K., and Pipeleers, D. G. (2011) Clusters of conserved beta cell marker genes for assessment of beta cell phenotype. [Erratum in *PLoS One* (2012);7.] *PLoS One* **6**, e24134
20. Dioum, E. M., Osborne, J. K., Goetsch, S., Russell, J., Schneider, J. W., and Cobb, M. H. (2011) A small molecule differentiation inducer increases insulin production by pancreatic β cells. *Proc. Natl. Acad. Sci. USA* **108**, 20713–20718
21. Szabat, M., Lynn, F. C., Hoffman, B. G., Kieffer, T. J., Allan, D. W., and Johnson, J. D. (2012) Maintenance of β-cell maturity and plasticity in the adult pancreas: developmental biology concepts in adult physiology. *Diabetes* **61**, 1365–1371
22. McKinnon, C. M., and Docherty, K. (2001) Pancreatic duodenal homeobox-1, PDX-1, a major regulator of beta cell identity and function. *Diabetologia* **44**, 1203–1214
23. Bernardo, A. S., Hay, C. W., and Docherty, K. (2008) Pancreatic transcription factors and their role in the birth, life and survival of the pancreatic beta cell. *Mol. Cell. Endocrinol.* **294**, 1–9
24. Schisler, J. C., Jensen, P. B., Taylor, D. G., Becker, T. C., Knop, F. K., Takekawa, S., German, M., Weir, G. C., Lu, D., Mirmira, R. G., and Newgard, C. B. (2005) The Nkx6.1 homeodomain transcription factor suppresses glucagon expression and regulates glucose-stimulated insulin secretion in islet beta cells. *Proc. Natl. Acad. Sci. USA* **102**, 7297–7302
25. Barbagallo, D., Condorelli, A. G., Piro, S., Parrinello, N., Fløyel, T., Ragusa, M., Rabuazzo, A. M., Størling, J., Purrello, F., Di Pietro, C., and Purrello, M. (2014) CEBPA exerts a specific and biologically important proapoptotic role in pancreatic β cells through its downstream network targets. *Mol. Biol. Cell* **25**, 2333–2341
26. Belo, J., Krishnamurthy, M., Oakie, A., and Wang, R. (2013) The role of SOX9 transcription factor in pancreatic and duodenal development. *Stem Cells Dev.* **22**, 2935–2943
27. Ebrahimie, M., Esmaeili, F., Cheraghi, S., Houshmand, F., Shabani, L., and Ebrahimie, E. (2014) Efficient and simple production of insulin-producing cells from embryonal carcinoma stem cells using mouse neonate pancreas extract, as a natural inducer. *PLoS One* **9**, e90885
28. Lilla, V., Webb, G., Rickenbach, K., Maturana, A., Steiner, D. F., Halban, P. A., and Irminger, J. C. (2003) Differential gene expression in well-regulated and dysregulated pancreatic beta-cell (MIN6) sublines. *Endocrinology* **144**, 1368–1379
29. Polak, M., Scharfmann, R., Seilheimer, B., Eisenbarth, G., Dressler, D., Verma, I. M., and Potter, H. (1993) Nerve growth factor induces neuron-like differentiation of an insulin-secreting pancreatic beta cell line. *Proc. Natl. Acad. Sci. USA* **90**, 5781–5785
30. Vidaltamayo, R., Sánchez-Soto, M. C., Rosenbaum, T., Martínez-Merlos, T., and Hiriart, M. (1996) Neuron-like phenotypic changes in pancreatic β-cells induced by NGF, FGF, and dbcAMP. *Endocrine* **4**, 19–26
31. Hutton, J. C., Christofori, G., Chi, W. Y., Edman, U., Guest, P. C., Hanahan, D., and Kelly, R. B. (1993) Molecular cloning of mouse pancreatic islet R-cadherin: differential expression in endocrine and exocrine tissue. *Mol. Endocrinol.* **7**, 1151–1160
32. Bonacci, T. M., Hirsch, D. S., Shen, Y., Dokmanovic, M., and Wu, W. J. (2012) Small GTPase Rho regulates R-cadherin through Dia1/profilin-1. *Cell. Signal.* **24**, 2102–2110
33. Emond, M. R., Biswas, S., Blevins, C. J., and Jontes, J. D. (2011) A complex of protocadherin-19 and N-cadherin mediates a novel mechanism of cell adhesion. *J. Cell Biol.* **195**, 1115–1121
34. Apostolopoulou, M., and Ligon, L. (2012) Cadherin-23 mediates heterotypic cell-cell adhesion between breast cancer epithelial cells and fibroblasts. *PLoS One* **7**, e33289
35. Wang, X., Xie, B., Qi, Y., Wallerman, O., Vasylovska, S., Andersson, L., Kozlova, E. N., and Welsh, N. (2016) Knock-down of ZBED6 in insulin-producing cells promotes N-cadherin junctions between beta-cells and neural crest stem cells in vitro. *Sci. Rep.* **6**, 19006
36. Halban, P. A., Powers, S. L., George, K. L., and Bonner-Weir, S. (1987) Spontaneous reassociation of dispersed adult rat pancreatic islet cells into aggregates with three-dimensional architecture typical of native islets. *Diabetes* **36**, 783–790
37. Hauge-Evans, A. C., Squires, P. E., Persaud, S. J., and Jones, P. M. (1999) Pancreatic beta-cell-to-beta-cell interactions are required for integrated responses to nutrient stimuli: enhanced Ca^{2+} and insulin secretory responses of MIN6 pseudoislets. *Diabetes* **48**, 1402–1408

Received for publication August 16, 2016.
Accepted for publication June 12, 2018.

w.fasebj.org by The University of British Columbia Library (142.103.160.110) on July 28, 2018. The FASEB Journal Vol. ${article.issue.getVolume()}, No. ${article.issue.getIssueNum